Available online at website: https://journal.bcrec.id/index.php/bcrec

Bulletin of Chemical Reaction Engineering & Catalysis, 19 (4) 2024, 599-608

Research Article

Preparation of a Novel ACS/CS/EDTA Composite from Sugarcane Bagasse for Enhanced Adsorption of Carbon Dioxide

Quang Minh Pham[1], Xuan Son Nghiem[2], Thang Le Minh[2], and Anh-Tuan Vu[2,*]

[1]Physico-chemical Department, National Institute for Control of Vaccine and Biologicals, Viet Nam
[2]School of Chemistry and Life Sciences, Hanoi University of Science and Technology, Hanoi, Viet Nam

Received: 31th October 2024; Revised: 12th November 2024; Accepted: 13th November 2024
Available online: 16th November 2024; Published regularly: December 2024

Abstract

This study presents a simple method for the production of activated carbon (ACS) from sugarcane bagasse. To increase the CO_2 adsorption efficiency, the ACS/CS/EDTA composite was prepared by modifying ACS with ethylenediaminetetraacetic acid (EDTA) and chitosan (CS). The as-prepared materials were characterized by X-ray Diffraction (XRD), Field Emission Scanning Electron Microscope (FE-SEM), Energy Dispersive X-ray Spectroscopy (EDS), High Resolution – Transmission Electron Microscope (HR-TEM), Fourier Transform Infra-Red (FT-IR), and N_2 adsorption/desorption isotherms. The obtained ACS is an amorphous and porous material and contains both micropores and mesopores. The micropore volume, mesopore volume, Brunauer–Emmett–Teller (BET) surface area and average pore width of the ACS are 0.112 cm^3/g, 0.193 cm^3/g, 354.8 m^2/g and 55.7 Å, respectively. The dispersion of EDTA and CS on the activated carbon leads to a deterioration of the structural properties while it increases the aggregation of the ACS/CS/EDTA composite. The performance of the materials was evaluated by CO_2 adsorption at ambient pressure. The effects of EDTA, adsorption temperature and gas composition were also investigated in detail. In addition, the durability of the composite was evaluated through the adsorption and desorption cycle.

Keywords: Activated carbon, Sugarcane bagasse, Carbon dioxide, Adsorption, EDTA

How to Cite: Pham, Q. M., Nghiem, X. S., Minh, T. L., Vu, A.-T. (2024). Preparation of a Novel ACS/CS/EDTA Composite from Sugarcane Bagasse for Enhanced Adsorption of Carbon Dioxide. *Bulletin of Chemical Reaction Engineering & Catalysis*, 19 (4), 599-608 (doi: 10.9767/bcrec.20239)

Permalink/DOI: https://doi.org/10.9767/bcrec.20239

1. Introduction

Sugarcane bagasse is the fibrous part of sugarcane after the juice has been squeezed out and is a by-product of sugar mills. The main components of sugarcane bagasse are fibers, water and a small amount of soluble substances. Sugarcane bagasse is in the form of fibers that are insoluble in water or other solvents. Normally, the sugarcane is disposed of as waste after the juice has been pressed, as it can no longer be used. In reality, however, bagasse has many uses and is used in many areas of life, e.g. as fertilizer, fuel, animal feed, pulp, decorative pots, for the production of plywood and for packaging products [1-3].

In recent years, Vietnam has been one of the largest sugarcanes producing countries in the world with an average production of 15 to 18 million tons/year. After the sugarcane is pressed to extract sugar, about 4.5 million tons of bagasse are produced annually. Sugarcane bagasse, which mainly contains cellulose (50 by weight), with the remainder consisting of hemicellulose (25 %) and lignin (25 %) [4], is considered an important raw material for the production of low-cost activated carbon, which helps to increase the value of sugarcane and reduce solid waste emissions.

* Corresponding Author.
Email: tuan.vuanh@hust.edu.vn (A. T. Vu)

The synthesis of activated carbon from sugarcane bagasse can be carried out by one-step pyrolysis in the presence of $ZnCl_2$, Na_2CO_3, NaOH, H_3PO_4, etc. [5]. These chemicals play an important role in preventing the formation of aromatic hydrocarbon macromolecules from lignin, lowering the temperature of lignin dehydration, and destroying the structural carbon network at high temperatures to form porous channels in the activated carbon [6]. The high-quality porous activated carbon was prepared from sugarcane bagasse by an implicit chemical activation method using $ZnCl_2$ as a chemical activator, the material showed fast adsorption kinetics and high adsorption capacity for diclofenac sodium (315 $mg.g^{-1}$) [7]. Activated carbon was prepared by pyrolyzed with KOH as a potential positive electrode catalyst for vanadium redox flow batteries sugarcane bagasse [8], the activated carbon showed mesoporous material with the surface area of 1255 m^2/g. The activated carbon produced from sugarcane bagasse with a large surface area (1500 m^2/g) and high porosity exhibited a high adsorption capacity for toxic chemicals [9]. The activated carbon prepared from sugarcane bagasse by physico-chemical activation in an acidic medium (H_3PO_4, 85 wt%) and subsequent activation at high temperature showed high removal of (Pb) and (Cu) at pH = 5, Q_{max} = 968.72 and 754.14 $mg.g^{-1}$, respectively [10].

We are currently facing a number of pressing global environmental problems, including climate change, the destruction of biodiversity, freshwater resources, the ozone layer and soils, and pollution from toxic and persistent organic substances. These problems are interlinked and all have a direct impact on human life and social development. Above all, climate change is always regarded as the hottest environmental issue, whether at the national or global level. Moreover, it is also seen as an important issue affecting the process of sustainable development worldwide. Scientists widely agree that the increased socio-economic development activities in many sectors such as energy, industry, transportation, agriculture and forestry in recent decades have increased the concentration of greenhouse gasses (N_2O, CH_4, CFCs, H_2S, and especially CO_2) in the atmosphere, leading to global warming and thus climate change [11]. Scientists and countries have tried to find alternative energy sources such as solar and wind energy. However, fossil fuels still make up a large part of the world's energy supply and cannot currently be completely replaced by other sources. As a results, a large amount of CO_2 and other harmful gasses emitted by factories and engines need to be removed before they are released into the environment [12].

In addition to research on metal oxide-based materials for CO_2 removal [13-16], activated carbon-based composites have also attracted a great deal of attention from scientists due to their mechanical and chemical stability and easy regeneration. The nitrogen doped porous carbon sponge synthesized using a hard template and physical activation was very efficient in adsorbing CO_2, the uptake was 2.16–2.50 $mmol.g^{-1}$ at 25 °C and 1 bar [17]. The novel Zn-doped activated carbon developed from liquid agricultural biomass was efficient in adsorbing CO_2, the adsorption capacity was 370.41 $mg.g^{-1}$ at 25 °C [18]. Microwave pyrolysis of waste biomass can be used to produce micro-mesoporous activated carbons, the role of textural properties for CO_2 was investigated and CO_2 adsorption of 4.1 and 2.8 $mmol.g^{-1}$ at 0 and 25 °C, respectively, was demonstrated [19]. Activated carbons were prepared from a lignocellulosic material, African palm shells (*Elaeis guineensis*), by chemical impregnation of the precursor with solutions of 1–7 % w/v $Cu(NO_3)_2$ and showed adsorption of CO_2 between 103 and 217 $mg.g^{-1}$ [20]. Activated carbon prepared from olive waste was used as an adsorbent for the capture of CO_2, the maximum adsorption capacity according to the Langmuir model (q_m) was 9.374 $cm^3.g^{-1}$ [21]. These investigations show that activated carbon itself has a low adsorption of CO_2. The Integration of activated carbon with metals, metal oxides or non-metallic elements can increase the CO_2 adsorption capacity. However, the functionalization of activated carbon with organic substances containing basic functional groups to interact with CO_2 is a mystery that researchers are still investigating. In this study, the activated carbon was produced from sugarcane bagasse. To increase CO_2 adsorption efficiency, the surface of the activated carbon was surface modified with EDTA and CS. The resulting composites were characterized and used to adsorb CO_2 at ambient pressure.

2. Materials and Method

2.1. Chemicals and Materials

The sugarcane bagasse was obtained from the province of Thanh Hoa in Vietnam. The chitosan was imported from China. Ethylenediaminetetraacetic acid (EDTA), sodium acetate trihydrate ($CH_3COONa.3H_2O$, 99%), isopropyl alcohol (99%), sodium hydroxide (NaOH, 99%), hydrochloric acid (HCl, 37%), acetic acid (CH_3COOH 2%), ammonium solution (NH_3, 28%) and the necessary chemicals were purchased from Merck. N_2 (99.99%) was used as purge gas during activation and regeneration in the cyclic test, CO_2 (99.99%) was used for the sorption test. Double distilled water was used for all experiments.

2.2. Preparation of ACS

Normally, 80 g of sugarcane bagasse was washed to remove sugar and sand and dried at 80 ºC for 8 h. The dried bagasse was ground to a fine powder and sieved with a mesh size of 1 mm, then mixed with 80 g of saturated NaOH solution. Subsequently, the paste mixture was dried and calcined anaerobically at 800 ºC for 60 min. After cooling, the product was ground in a porcelain mortar and sieved to obtain a particle size of 0.7 mm, and then it was mixed with 1 M HCl solution in excess for 1 day to allow the reaction to complete. The product was then filtered, washed with distilled water and dried at 150 ºC for 10 h to obtain activated carbon powder and denoted as (ACS).

2.3. Preparation of ACS/CS/EDTA composite

Two 100 mL beakers were prepared. Beaker A: 0.1 g of chitosan was accurately weighed into a 100 mL beaker containing 10 mL of 2% CH_3COOH. The mixture was stirred with a magnetic stirrer for 12 h to completely dissolve the chitosan. Beaker B: 0.2 g of ACS was accurately weighed into a 100 mL beaker containing 20 mL of isopropyl alcohol, and then stirred at 70 ºC for 5 min, as presented in Figure 1(a). Beaker B was poured into beaker A. The solution was stirred at 70 ºC for 60 min to allow the chitosan to adhere to the ACS. Then 10 mL of EDTA solution was slowly added to the mixture and stirred gradually until the EDTA was evenly distributed on the surface of the ACS. The mixture was filtered using a Buchner funnel and then washed several times with distilled water. The resulting solid was dried at 80 ºC for 12 h to obtain the ACS/CS/EDTA composite, as presented in Figure 1(b).

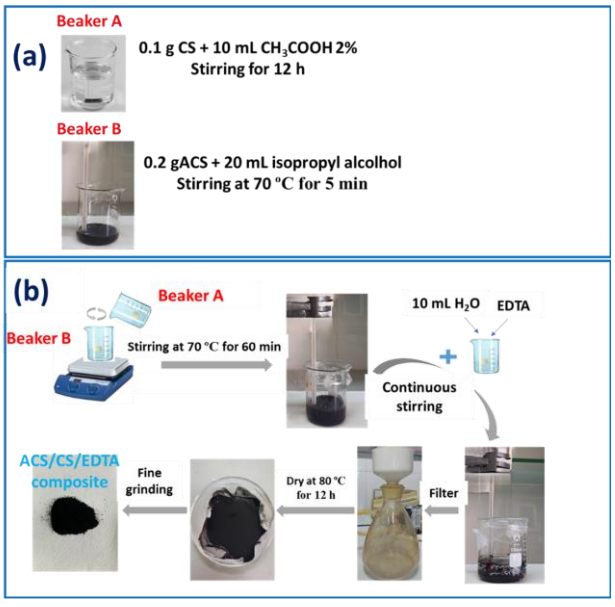

Figure 1. The scheme of preparation of ACS/CS/EDTA composite

2.4. Characterizations

The crystalline phase of sample was investigated by X-ray power diffraction (XRD). XRD patterns were obtained by using Bruker D8 Ax XRD-diffractometer (Germany) with Cu-Kα irradiation (40 kV, 40 mA). The 2θ ranging from 10 to 90° was selected to analyses the crystal structure. The morphology and size of the samples were observed field emission scanning electron microscopy (FE-SEM, JEOL-7600F). Textural properties were measured via N_2 sorption/desorption isotherms using a Quantachrome instrument (Autosorb iQ, version 3.0 analyzer). The specific surface area, pore volume and pore diameter were obtained by using the Brunauer-Emmett-Teller (BET) method.

2.4. CO_2 adsorption test

The CO_2 adsorption/desorption was performed in the thermogravimetric analyzer (TGA, Versa Thermal Instrument), as shown in Figure 2. The TGA system has a temperature range up to 1000 ºC, a capacity of 1.0 gram, a sensitivity of 0.2 ug and an accuracy of 0.1%. The balance operates on the zero-balance principle and uses a highly sensitive transducer coupled with a tout-band suspension system to detect minute changes in sample mass.

Normally, a sample quantity of 0.1 g was added to the sample container. Prior to CO_2 sorption, the prepared samples were activated at 150 °C in an N_2 stream of 30 mL.min^{-1} for 1 h to remove moisture, solvent and other adsorbates. The sample was then cooled to the sorption temperature and the N_2 gas stream was replaced by a CO_2 stream of 20 mL.min^{-1}. The mass of adsorbent increased due to the sorption of CO_2. As it approached saturation, the weight increase was caused by the CO_2 adsorbed on the sample and calculated by the following Equation [14].

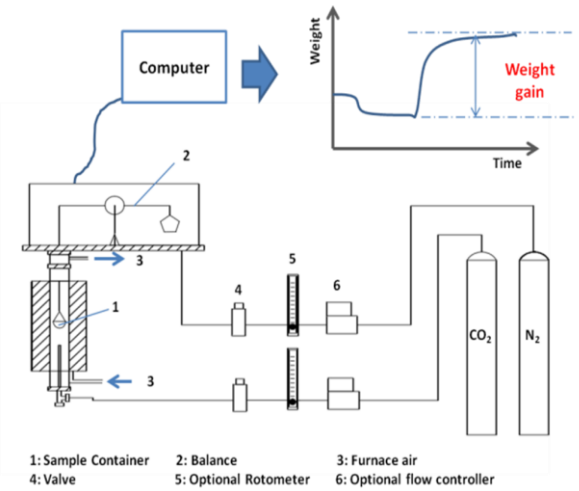

Figure 2. TGA structure and process

$$CO_2\ Adsorption\ (\%) = \frac{Weight\ of\ Adsorbed\ CO_2}{Weight\ of\ Adsorbent} \times 100\% \quad (1)$$

3. Results and Discussion

3.1. Characterization

The results of the XRD analysis of the ACS and ACS/CS/EDTA materials are shown in Figure 3. The XRD spectra of the two samples are almost identical, which proves that the ACS material does not change its structure after surface functionalization. In addition, both samples are characterized by a diffraction peak with a large half spectrum at 25°. The broad peak proves that the activated carbon produced from bagasse is amorphous. In the XRD spectrum of the ACS/CS/ETDA composite, the peaks at 33.55 and 44.73°, corresponding to (511) and (224) planes, respectively, are small, and indicate crystalline EDTA (JCPDS 27-1927). This partly due to the uniform distribution of EDTA on the surface of ACS [22], but may also be due to obscuration by the peak of ACS. Furthermore, the absence of the CS peak proves that it is present in amorphous form and acts as a bridge between ACS and EDTA.

The SEM results of ACS and ACS/CS/EDTA are shown in Figure 4. ACS has a honeycomb structure, a homogeneous surface with closely connected thin layers forming a fine porous network. SEM images at different magnifications (5 µm, 1 µm, and 500 nm) show that the surface of the ACS sample has many very small, evenly distributed pores in Figure 4(a-c). This indicates that ACS can provide a large surface area, which is advantageous for applications requiring high adsorption capacity. ACS/CS/EDTA, on the other hand, has a more complex structure, with large blocks and irregular loose sheets. SEM images of this sample at magnifications of 10 µm and 5 µm show the presence of pores with deep grooves and distinct voids. The pores of the composite are not only smaller but also unevenly distributed, resulting in a rough surface in Figure 4(d-e). This shows that the combination of EDTA and CS with ACS in the sample has changed the surface structure and created more active sites that increase the CO_2 adsorption capacity. This change is important for optimizing the material surface for applications in the adsorption process.

The elemental composition of the ACS/CS/EDTA composite was analyzed by EDS spectrum. Figure 4(g) shows that the composite contains 93.3 wt% C, which is the largest proportion in the sample; 6.3 wt% O, 0.2 wt% Na, 0.2 wt% Si. The presence of Na may be due to EDTA. However, N was not detected due to the detection limit of the EDS method. The presence of C in a high proportion (93.3%) indicates that CS was tightly bound to the ACS surface. Although N, an important component of CS and EDTA, was not detected, the presence of oxygen (O) at 6.3 % can indicate that EDTA was functionalized and dispersed on the material surface.

The HR-TEM image of the ACS/CS/EDTA composite shows a complex microstructure (Figure 5). At low magnification, the image shows clusters of particles with a heterogeneous structure, including unevenly sized particles and irregularly shaped thin layers stacked on top of each other, as seen in Figure 5(a, b). Upon closer inspection of Figure 5. (c, d), the crystals show tight aggregation with dark and light areas

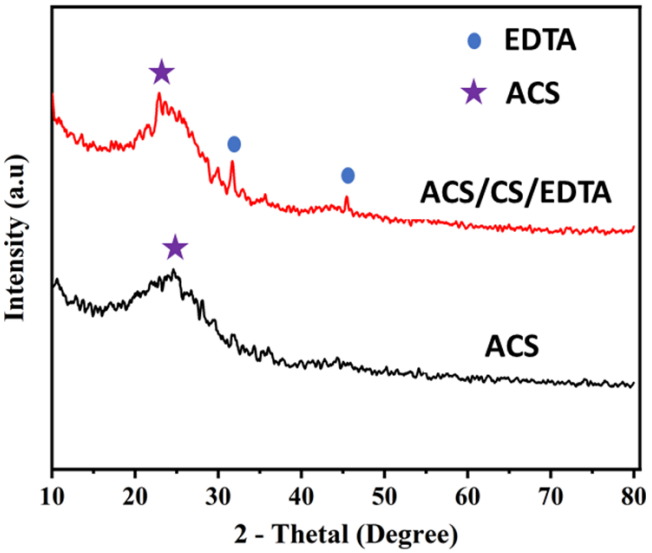

Figure 3. XRD pattern of ACS and ACS/CS/EDTA composite.

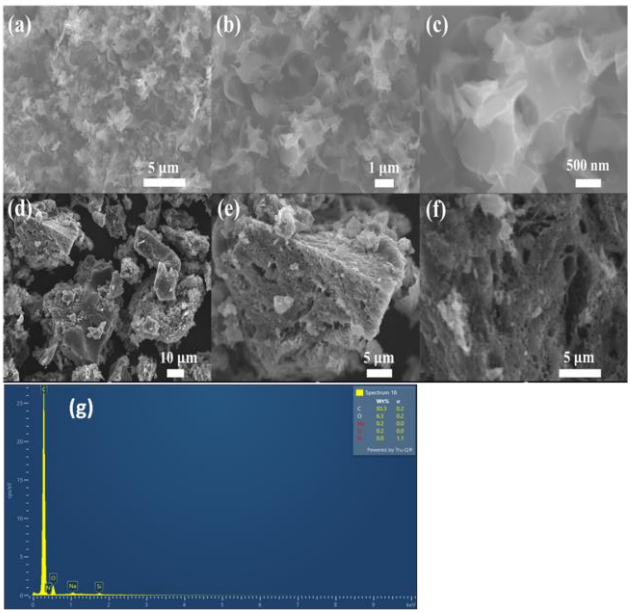

Figure 4. SEM images of (a-c) ACS and (d-f) ACS/CS/EDTA; (g) EDS spectrum of ACS/CS/EDTA.

reflecting the uneven distribution of components, indicating strong binding between EDTA, chitosan and ACS in the composite structure. At higher magnification Figure 5. (e, f), the layers are arranged in an ordered fashion. The characteristic interlayer distance for EDTA was calculated to be 0.595 nm, suggesting that EDTA may be present in the crystal phase. This complex association between different phases may contribute to the adsorption capacity of the composite.

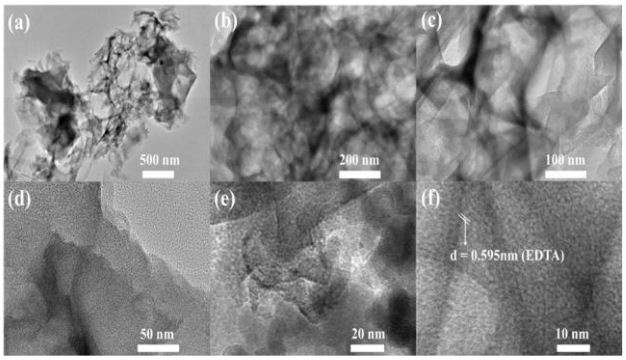

Figure 5. HR-TEM images of ACS/CS/EDTA.

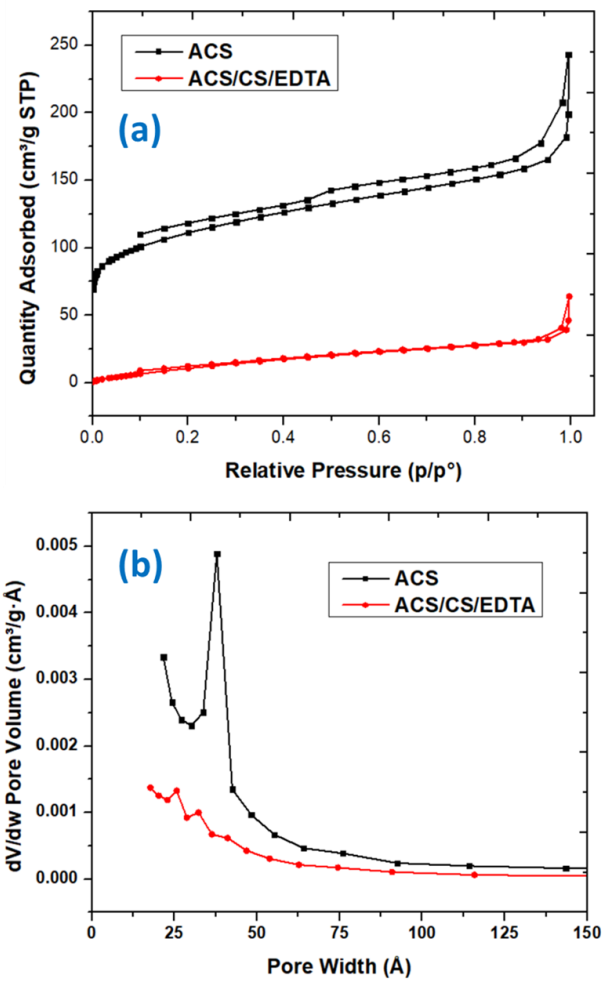

Figure 7. (a) N_2 adsorption/desorption isotherms and (b) pore size distribution of ACS and ACS/CS/EDTA.

Figure 6 shows the FT-IR spectra of the ACS and AC/CS/EDTA samples. The appearance of absorption peaks at 3274 cm^{-1} in the spectra of both material samples is due to hydrogen bond (O–H), phenolic hydroxyl or N–H stretching vibrations [23]. In particular, the intensity peak at 3274 cm^{-1} in the FT-IR spectrum of AC/CS/EDTA is significantly enhanced, indicating that the number of hydrogen bonds is increased after modification by EDTA and CS (–OH bonds in EDTA and CS molecules). The peaks at 1570 cm^{-1} can be assigned to the N–H deformation vibration, phenolic hydroxyl, C=C or C=O stretching vibration [24]. In the FT-IR spectra of the AC/CS/EDTA composite, the intensity of this peak was significantly enhanced, indicating the occurrence of the C=O and N–H stretching vibrations of EDTA and CS, respectively. The peaks at 890 cm^{-1} can be assigned to the C–H stretching vibrations. In addition, the absorption peaks at 2094, 1370 and 1016 cm^{-1} are characteristic of N–H, C–N and C–O bonds in EDTA and CS molecules, respectively [23, 24]. The absorption peaks of the pure AC and the AC/CS/EDTA composite are almost identical, indicating that the modification with EDTA and CS does not change the original chemical properties of the pure AC material. However, the increased peak intensities and the appearance of new absorption peaks in the FT-IR spectra of the composite indicate that the EDTA and CS molecules are dispersed and crystallized on the surface of the pure ACS.

The textural properties of the sample are shown in Figure 7. Pure ACS exhibits a diverse N_2 adsorption/desorption isotherm. The part of the curve corresponding to p/p_o 0-0.5 is of type I, attributed to microporous material, and the remaining part of the curve, p/p_o 0.5-1.0, is of type 4 with a type H4 hysteresis loop (Figure 7(a)) attributed to the IUPAC classification and often

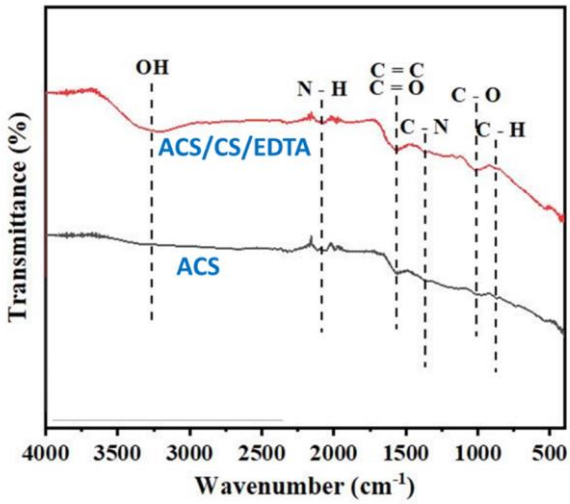

Figure 6. FT-IR spectra of ACS and ACS/CS/EDTA

associated with narrow slit pores. The pore size distribution of the composite concentrates in the range of 30-40 Å (Figure 7(b). As seen in Table 1, the micropore volume and mesopore volume are 0.112 and 0.193 $cm^2.g^{-1}$, the BET surface area and average pore width are 354.8 $m^2.g^{-1}$ and 55.7 Å, respectively. The N_2 adsorption isotherm was lower and the hysteresis loop of the ACS/CS/EDTA composite was smaller than that of AC. The pore size distribution of the composite is not concentrated. The micropore volume, mesopore volume, BET surface area and average pore width are 0.008 $cm^3.g^{-1}$, 0.062 $cm^3.g^{-1}$, 54.8 $m^2.g^{-1}$ and 47.1 Å, respectively. The decrease in the textural properties of the composite can be attributed to the dispersion and blocking of the pores in ACS by EDTA and CS molecules.

3.2. CO_2 adsorption

The results of the CO_2 adsorption studies of ACS and ACS/CS/EDTA composite are shown in Figure 8. The CO_2 is adsorbed slowly on ACS, achieving an adsorption rate of only 2.81 wt.% in 120 min, although ACS is a porous structure material with a large surface area, as shown above. This demonstrates that CO_2 interacts only weakly with the surface of the activated carbon synthesized from sugarcane bagasse. While the CO_2 adsorption rate on the ACS/CS/EDTA composite is very fast in the first 20 min, the adsorption of 13.09 wt.%, the adsorption increases slightly thereafter and reaches saturation after 120 min, resulting in a CO_2 adsorption capacity of 18.28 wt.%. The improvement in adsorption can be attributed to the uniform dispersion of EDTA on the surface of ACS and the interaction of CO_2 with the N-containing functional groups in EDTA and CS. The surface area and pore volume do not play a decisive role in CO_2 adsorption.

To investigate the effect of EDTA content on the adsorption capacity of composites, the ratio of EDTA : AC was veried from 0.25 to 1. The samples were labeled as ACS/CS/EDTA-X, where X stands

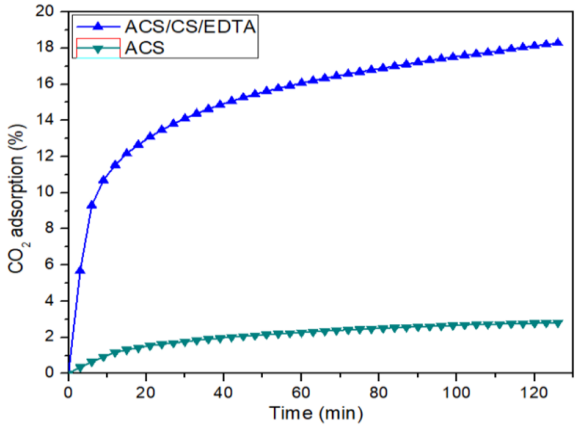

Figure 8. CO_2 adsorption on the ACS and ACS/CS/EDTA samples.

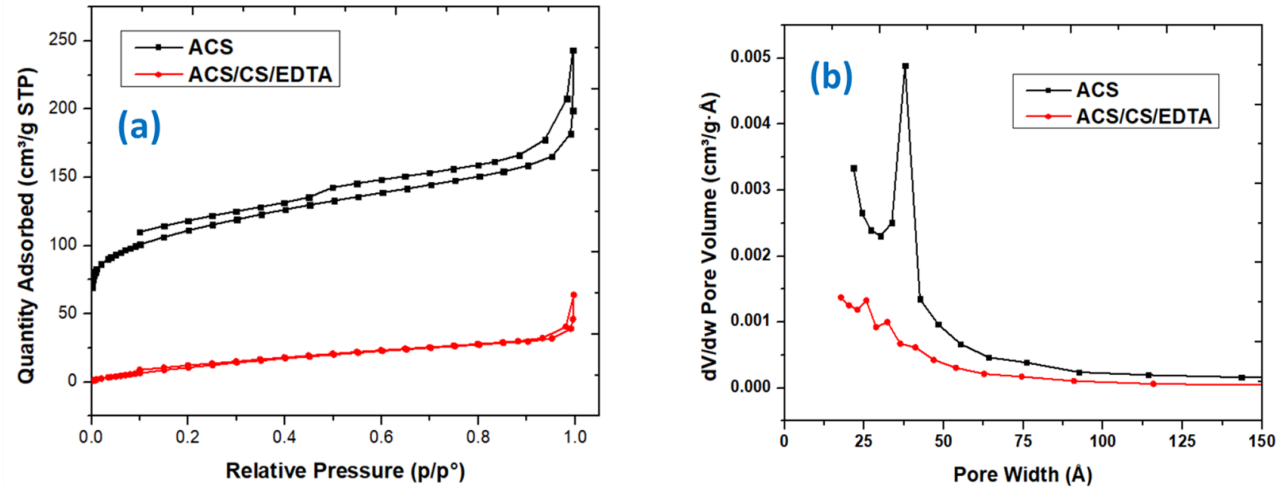

Figure 7. (a) N_2 adsorption/desorption isotherms and (b) pore size distribution of ACS and ACS/CS/EDTA.

Table 1. Textural properties of ACS and ACS/CS/EDTA.

Samples	BET surface area ($m^2.g^{-1}$)	Micropore Area area ($m^2.g^{-1}$)	External surface area ($m^2.g^{-1}$)	Micropore volume ($cm^3.g^{-1}$)	Mesopore volume ($cm^3.g^{-1}$)	Average pore width (Å)
ACS	354.8	259.3	145.5	0.112	0.193	55.7
ACS/CS/EDTA	54.8	19.2	35.6	0.008	0.062	47.1

for the ratio of EDTA. The result is presented in Figure 9. When the ratio is 0.25, the adsorption occurs rapidly in the first 20 min, the amount of adsorbed CO_2 is 8.26 wt.%, then the adsorption increases slightly and reaches saturation after 120 min, the adsorption capacity reaches 11.6 wt.%. When the ratio increases to 0.5, the adsorption capacity of the composite increases significantly. After 20 min the adsorption amount is 13.09 wt.% and after 120 min the adsorption capacity is 18.28 wt.%. This proves the role of EDTA in increasing the adsorption capacity of CO_2, This is in good agreement with previous studies on amine-modified activated carbon for CO_2 adsorption [25,26]. However, as the ratio increases further, the CO_2 adsorption decreases, which may be due to the uneven dispersion of EDTA on the surface of the activated carbon when the its concentration is high. The CO_2 adsorption capacity of the composite at ratio 1 decreases to 12.60 and 16.42 wt.% after 20 and 120 min, respectively.

To study the effect of temperature on CO_2 adsorption, in this study, the temperature was varied from 25 to 150 °C. The results are presented in Figure 10. As the temperature increases, the adsorption of CO_2 decreases. In the first 20 min, the CO_2 adsorption rate at 50 °C is slightly higher than at 25 °C, however, the adsorption capacity at 25 °C is higher than at 50 °C. When the temperature increases further, CO_2 adsorption significantly decreases. At 150 °C, the amount of adsorbed CO_2 was 0.97 wt.% in the first 20 min and after 120 min the adsorption capacity remained almost unchanged. This proves that adsorption is an exothermic process and increasing the temperature can reduce adsorption of CO_2 on composite. This is in complete agreement with previous studies on solid materials modified by amine for CO_2 adsorption [27,28].

To investigate the effect of gas composition on CO_2 adsorption, the feed gas was varied from 100% CO_2 to 30% CO_2 and 10% CO_2. The results are shown in Figure 11. The results show that the gas composition has a significant influence on the adsorption rate and efficiency. As the CO_2 content decreases, the rate and adsorption capacity also decrease. For pure CO_2, the adsorption at 20 min and the adsorption capacity at 120 min are 13.09 and 18.28 wt.% respectively. These values are decrease to 11.63 and 16.50 wt.%, 8.31 and 15.84 wt.% corresponding to a CO_2 content of 30 and 10 %. However, the CO_2 adsorption rate in wet condition is faster in the first 20 min compared to the dry state, the amount of CO_2 adsorption reaches15.49 wt.% after 20 min. Thereafter, adsorption only slightly increases and it reaches saturation after 120 min. The adsorption capacity in the wet state is still lower than in the dry condition, showing the sorption capacity of 17.67 wt.%. This can be attributed to the reaction of CO_2 with water to form H_2CO_3, which tends to adsorb

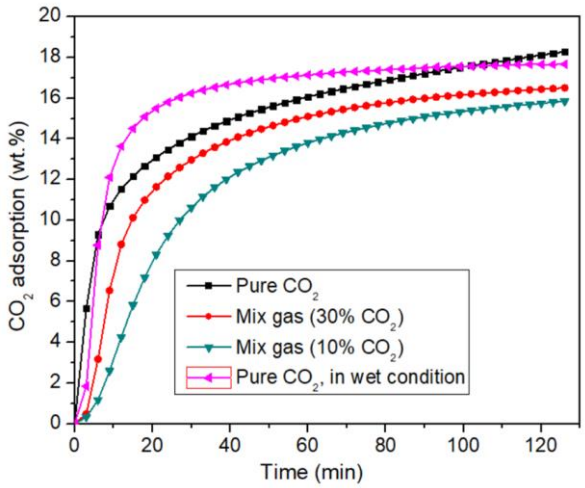

Figure 11. Effect of gas component on CO_2 adsorption.

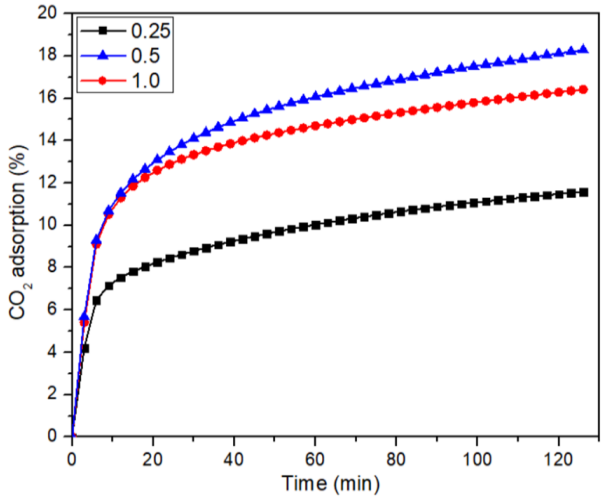

Figure 9. Effect of EDTA content on CO_2 adsorption.

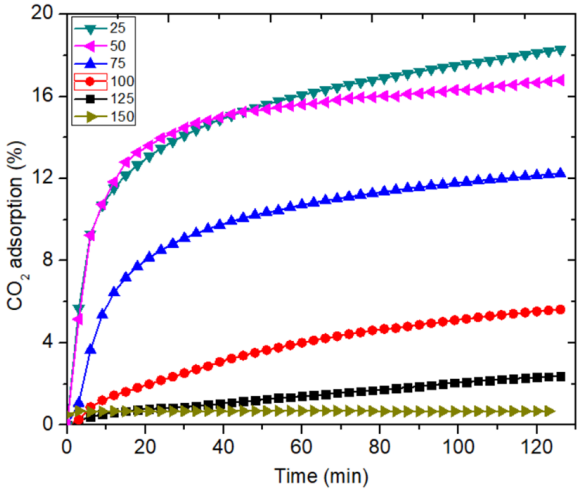

Figure 10. Effect of temperature on CO_2 adsorption.

rapidly to the nitrogen functional groups in EDTA and CS. However, due to the limited active sites, the maximum adsorption capacity is not greater than that under dry condition.

As can be seen from the results in Figure 8, the ACS/CS/EDTA composite shows the rapid adsorption in initial 20 min. The adsorption capacity corresponds to 71.61 % of the saturation capacity within 120 min at 25 °C. With regard to the reproduction of CO_2 capture, fast cyclic operation is desirable. However, in this study, cyclic CO_2 sorption/desorption tests were conducted under accelerated test conditions (short sorption and desorption times) to evaluate the stability of ACS/CS/EDTA. Adsorption of pure CO_2 was performed at 25 °C for 20 min and regeneration with an N_2 flow was carried out at 300 °C for 30 min to complete the desorption of CO_2 (Figure 12). The ACS/CS/EDTA composite proves to be relatively stable in the adsorption/desorption of CO_2. The sorption capacity of ACS/CS/EDTA at the 10th cycle is 12.22 wt.%, which is 94.6 % of the capacity at the first adsorption. This shows that the ACS/CS/EDTA composite is stable 10 times at the activation temperature of 300 °C and the regeneration temperature of 300 °C and can be a potential material for application in CO_2 capture.

4. Conclusion

The activated carbon successfully synthesized from sugarcane bagasse proves to be a porous and amorphous material. The activated carbon has a surface area of 354.8 $m^2.g^{-1}$ and contains both micropores and mesopores with the values of 0.112 and 0.193 $cm^3.g^{-1}$, respectively. ACS has a low adsorption capacity of only 2.81 wt.% after 120 min. The novel ACS/CS/EDTA composite was prepared by modifying the surface of ACS by EDTA and CS. This leads to reduce the textural properties of the ACS/CS/EDTA composite. The surface area, micropore volume and mesopore volume are 54.8 $m^2.g^{-1}$, 0.008 $cm^3.g^{-1}$ and 0.062 $cm^3.g^{-1}$, respectively. However, this does not reduce the CO_2 adsorption of the composite. The nitrogen-containing functional groups are able to interact with CO_2 and can increase the adsorption rate and capacity. At optimum EDTA:ACS ratio is 0.5, the ACS/CS/EDTA shows rapid adsorption in the initial stage. The amount of adsorbed CO_2 is 13.09 wt.% in the initial 20 min and reaches saturation after 120 min with an adsorption capacity of 18.28 wt.%. The adsorption capacity of composite decreases with increasing temperature. At 150 °C, the adsorption capacity is only 0.97 wt.%, which proves that the adsorption process is exothermic and desorption can take place at medium temperature. It is proven that the gas composition influences the adsorption. The lower the CO_2 content in the input gas, the lower the adsorption. In addition, the presence of moisture increases the adsorption rate in the initial stage, which can be explained by the formation of a weak acid H_2CO_3 that quickly interacts with basic, nitrogen-containing functional groups. However, the presence of water does not increase the adsorption capacity throughout the process. The adsorption capacity under wet conditions reached 17.67 wt.%, which is lower than that under dry condition. In addition, the stability of the ACS/CS/EDTA composite is demonstrated by the adsorption/desorption cycle experiment. The adsorption capacity at the 10th cycle is 94.6% compared to the first time. This proves that the ACS/CS/EDTA composite has the potential to capture CO_2 from flue gas.

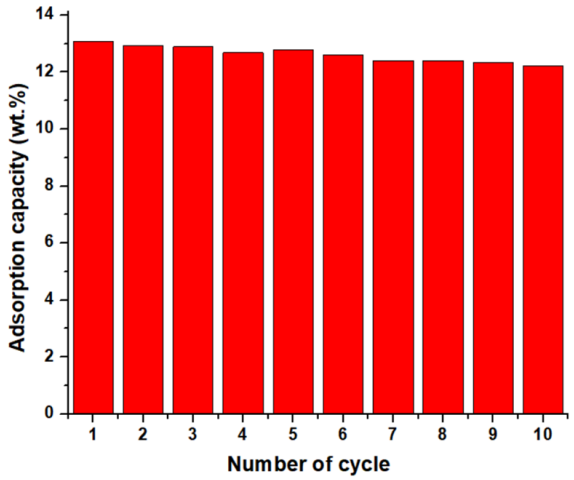

Figure 12. Cyclic test temperature profile and sorption capacity of ACS/CS/EDTA composite operated by sorption at 25 °C and regeneration at 350 °C; pure CO_2 sorption and N_2 regeneration.

Acknowledgments

This study was funded from the Project on training and fostering scientific and technological human resources domestically and abroad using the national budget of the Ministry of Science and Technology of Vietnam. Code: 2395.

CRediT Authors Statement

Quang Minh Pham: Methodology, investigation, resources, experiment, and writing draft; Xuan Son Nghiem and Minh Thang Le preparation of activated carbon from sugarcane bagasse, investigation and experiment; Anh-Tuan Vu: Review, editing, and validation. All authors have read and agreed to the published version of the manuscript.

References

[1] Iwuozor, K.O., Adeniyi, A.G., Emenike, E.C., Ojeyemi, T., Egbemhenghe, A.U., Okorie, C.J., Ayoku, B.D., Saliu, O.D. (2023) Prospects and challenges of utilizing sugarcane bagasse as a bio-coagulant precursor for water treatment, *Biotechnology Reports*. 39, e00805. DOI: 10.1016/j.btre.2023.e00805.

[2] Zafeer, M.K., Menezes, R.A., Venkatachalam, H., Bhat, K.S. (2024) Sugarcane bagasse-based biochar and its potential applications: a review, *Emergent Materials*. 7 (1), 133-161. DOI: 10.1007/s42247-023-00603-y.

[3] Ajala, E.O., Ighalo, J.O., Ajala, M.A., Adeniyi, A.G., Ayanshola, A.M. (2021) Sugarcane bagasse: a biomass sufficiently applied for improving global energy, environment and economic sustainability, *Bioresources and Bioprocessing*. 8 (1), 87. DOI: 10.1186/s40643-021-00440-z.

[4] Kamboj, A., Sadh, P.K., Yadav, B., Kumari, A., Kumar, R., Surekha, Saharan, B.S., Brar, B., Kumar, D., Goyal C., Duhan, J.S. (2024) Unravelling the potential of sugarcane bagasse: An eco-friendly and inexpensive agro-industrial waste for the production of valuable products using pretreatment processes for sustainable bio-economy, *Journal of Environmental Chemical Engineering*. 12(6), 114461. DOI: 10.1016/j.jece.2024.114461.

[5] Kakom, S.M., Abdelmonem, N.M., Ismail, I.M., Refaat, A.A. (2023) Activated Carbon from Sugarcane Bagasse Pyrolysis for Heavy Metals Adsorption, *Sugar Tech*. 25(3), 619-629. DOI: 10.1007/s12355-022-01214-3.

[6] Kilic, M., Apaydın-Varol, E., Pütün, A. (2012) Preparation and surface characterization of activated carbons from Euphorbia rigida by chemical activation with $ZnCl_2$, K_2CO_3, NaOH and H_3PO_4, *Applied Surface Science*. 261, 247–254. DOI: 10.1016/j.apsusc.2012.07.155.

[7] Abo El Naga, A.O., El Saied, M., Shaban, S.A., El Kady, F.Y. (2019) Fast removal of diclofenac sodium from aqueous solution using sugar cane bagasse-derived activated carbon, *Journal of Molecular Liquids*. 285, 9-19. DOI: 10.1016/j.molliq.2019.04.062.

[8] Mahanta, V., Raja, M., Kothandaraman, R. (2019) Activated carbon from sugarcane bagasse as a potential positive electrode catalyst for vanadium redox flow battery, *Materials Letters*. 247, 63-66. DOI: 10.1016/j.matlet.2019.03.045.

[9] Tran, T., Phạm, V.T., Quynh, B., Thanh Cong, H., Tam, D., Thuan, V., Bach, L.G. (2016) Production of Activated Carbon from Sugarcane Bagasse by Chemical Activation with ZnCl2: Preparation and Characterization Study, *Research Journal of Chemical Sciences*. 6, 42-47.

[10] Licona-Aguilar, Á.I., Torres-Huerta, A.M., Domínguez-Crespo, M.A., Palma-Ramírez, D., Conde-Barajas, E., Negrete-Rodríguez, M.X.L., Rodríguez-Salazar, A.E., García-Zaleta, D.S. (2022) Reutilization of waste biomass from sugarcane bagasse and orange peel to obtain carbon foams: Applications in the metal ions removal, *Science of The Total Environment*. 831, 154883. DOI: 10.1016/j.scitotenv.2022.154883.

[11] Lomax, G., Workman, M., Lenton, T., Shah, N. (2015) Reframing the policy approach to greenhouse gas removal technologies, *Energy Policy*. 78(0), 125-136. DOI: 10.1016/j.enpol.2014.10.002.

[12] Kang, S.H., Islam, F., Kumar Tiwari, A. (2019) The dynamic relationships among CO_2 emissions, renewable and non-renewable energy sources, and economic growth in India: Evidence from time-varying Bayesian VAR model, *Structural Change and Economic Dynamics*. 50, 90-101. DOI: 10.1016/j.strueco.2019.05.006.

[13] Vu, A.-T., Park, Y., Jeon, P.R., Lee, C.-H. (2014) Mesoporous MgO sorbent promoted with KNO_3 for CO_2 capture at intermediate temperatures, *Chemical Engineering Journal*. 258, 254-264. DOI: 10.1016/j.cej.2014.07.088.

[14] Vu, A.-T., Ho, K., Jin, S., Lee, C.-H. (2016) Double sodium salt-promoted mesoporous MgO sorbent with high CO_2 sorption capacity at intermediate temperatures under dry and wet conditions, *Chemical Engineering Journal*. 291, 161-173. DOI: 10.1016/j.cej.2016.01.080.

[15] Zeng, P., Zhao, C., Liang, C., Li, P., Zhang, H., Wang, R., Guo, Y., Xia, H., Sun, J. (2023) Comparative study on low-temperature CO_2 adsorption performance of metal oxide-supported, graphite-casted K_2CO_3 pellets, *Separation and Purification Technology*. 306, 122608. DOI: 10.1016/j.seppur.2022.122608.

[16] Chang, C.-W., Kao, Y.-H., Shen, P.-H., Kang, P.-C., Wang, C.-Y. (2020) Nanoconfinement of metal oxide MgO and ZnO in zeolitic imidazolate framework ZIF-8 for CO_2 adsorption and regeneration, *Journal of Hazardous Materials*. 400, 122974. DOI: 10.1016/j.jhazmat.2020.122974.

[17] Cui, H., Xu, J., Yan, N., Yan, R., Shi, J., Weng, Y. (2024) Synthesis of nitrogen enriched porous carbon sponge with the assistance of hard template and physical activation for highly efficient CO_2 adsorption, *Journal of Environmental Chemical Engineering*. 12(5), 113808. DOI: 10.1016/j.jece.2024.113808.

[18] Mechnou, I., Meskini, S., Elqars, E., Ait El Had, M., Hlaibi, M. (2024) Efficient CO_2 capture using a novel Zn-doped activated carbon developed from agricultural liquid biomass: Adsorption study, mechanism and transition state, *Surfaces and Interfaces*. 52, 104846. DOI: 10.1016/j.surfin.2024.104846.

[19] Durán-Jiménez, G., Rodriguez, J., Stevens, L., Kostas, E.T., Dodds, C. (2024) Microwave pyrolysis of waste biomass and synthesis of micro-mesoporous activated carbons: The role of textural properties for CO_2 and textile dye adsorption, *Chemical Engineering Journal*. 488, 150926. DOI: 10.1016/j.cej.2024.150926.

[20] Acevedo, S., Giraldo, L., Moreno-Piraján, J.C. (2020) Adsorption of CO_2 on Activated Carbons Prepared by Chemical Activation with Cupric Nitrate, *ACS Omega*. 5(18), 10423-10432. DOI: 10.1021/acsomega.0c00342.

[21] Jedli, H., Almonnef, M., Rabhi, R., Mbarek, M., Abdessalem, J., Slimi, K. (2024) Activated Carbon as an Adsorbent for CO_2 Capture: Adsorption, Kinetics, and RSM Modeling, *ACS Omega*. 9(2), 2080-2087. DOI: 10.1021/acsomega.3c02476.

[22] Nguyen, V.D., Cuong, V.T., Nguyen, T.H., Do, T.X., Vu, A.-T. (2024) Preparation of novel CS/SiO_2-EDTA nanocomposite from ash of rice straw pellets for enhanced removal efficiency of heavy metal ions in aqueous medium, *Journal of Water Process Engineering*. 60, 105175. DOI: 10.1016/j.jwpe.2024.105175.

[23] Liu, Y., Liu, X., Dong, W., Zhang, L., Kong, Q., Wang, W. (2017) Efficient adsorption of sulfamethazine onto modified activated carbon: a plausible adsorption mechanism, *Scientific Reports*. 7(1), 12437. DOI: 10.1038/s41598-017-12805-6.

[24] Ghamsari, M., Madrakian, T. (2019) Highly fast and efficient removal of some cationic dyes from aqueous solutions using sulfonated-oxidized activated carbon, *Analytical Bioanalytical Chemistry Research*. 6(1), 157-169. DOI: 10.22036/ABCR.2018.145499.1242.

[25] Gholidoust, A., Atkinson, J.D., Hashisho, Z. (2017) Enhancing CO_2 Adsorption via Amine-Impregnated Activated Carbon from Oil Sands Coke, *Energy & Fuels*. 31 (2), 1756-1763. DOI: 10.1021/acs.energyfuels.6b02800.

[26] Yang, Y., Liu, Y., Liu, S., Zhao, Y., Zhang, Q., Su, L., Chen, Z., Zhao, M. (2024) Experimental and theoretical investigation of amine-modified biomass-derived activated carbon for CO_2 capture: The effects of carbon chain length and types of amine. *Chemical Engineering Science*. 292, 119968. DOI: 10.1016/j.ces.2024.119968.

[27] Ismail, M.F.H., Masri, A.N., Mohd Rashid, N., Ibrahim, I.M., Mohammed, S.A.S., Yahya, W.Z.N. (2024) A review of CO_2 capture for amine-based deep eutectic solvents, *Journal of Ionic Liquids*. 4(2), 100114. DOI: 10.1016/j.jil.2024.100114.

[28] Waseem, M., Al-Marzouqi, M., Ghasem, N. (2023) A review of catalytically enhanced CO_2-rich amine solutions regeneration. *Journal of Environmental Chemical Engineering*. 11(4), 110188. DOI: 10.1016/j.jece.2023.110188.